

# Fracture toughness and strength of $\text{Al}_2\text{O}_3\text{-Y}_3\text{Al}_5\text{O}_{12}$ and $\text{Al}_2\text{O}_3\text{-Y}_3\text{Al}_5\text{O}_{12}\text{-ZrO}_2$ directionally solidified eutectic oxides up to 1900 K

J.Y. Pastor, J. LLorca, A. Martin, J.I. Pena, P.B. Oliete

*Departamento de Ciencia de Materiales, Universidad Politécnica de Madrid and Instituto Madrileño de Estudios Avanzados en Materiales (IMDEA-Materiales), E. T. S. de Ingenieros de Caminos, 28040 Madrid, Spain  
Instituto de Ciencia de Materiales de Aragón C.S.I. C., Universidad de Zaragoza, 50018 Zaragoza, Spain*

## Abstract

Ceramics rods of binary ( $\text{Al}_2\text{O}_3\text{-Y}_3\text{Al}_5\text{O}_{12}$ ) and ternary ( $\text{Al}_2\text{O}_3\text{-Y}_3\text{Al}_5\text{O}_{12}\text{-ZrO}_2$ ) eutectic ceramic oxides were grown in air and nitrogen using the laser-heated floating zone method. Both materials presented a fine and homogeneous microstructure, free from defects, with an average interlamellar spacing of 1.1 and 0.7  $\mu\text{m}$  for the binary and ternary eutectics, respectively. The strength and the toughness of the rods were measured from ambient temperature up to 1900 K by three-point bending. For the fracture tests, a sharp notch was introduced in the rods using a femto second-pulsed laser. Samples grown in nitrogen presented higher strength than those grown in air. The mechanical properties of the  $\text{Al}_2\text{O}_3\text{-YAG}$  binary eutectic did not change with a temperature up to 1500–1600 K and plastic deformation above this temperature led to a slight reduction in strength and an increase in toughness. In the case of the ternary eutectic, the toughening effect of the thermal residual stresses disappeared at high temperature and the toughness decreased by a factor of two at 1473 K. The behavior of the ternary eutectic above this temperature followed the trends of the binary one although the changes in strength and toughness were much larger because of the smaller domain size (which favored diffusion-assisted plastic flow) and the lower eutectic temperature.

**Keywords:** Microstructure-final; Strength; Fracture;  $\text{ZrO}_2\text{-Al}_2\text{O}_3\text{-Y}_2\text{O}_3$ ; Directionally solidified eutectic oxides

## 1. Introduction

$\text{Al}_2\text{O}_3$ -based directionally solidified eutectic oxides (DSEO) stand out as materials for very high temperature structural applications. As detailed in a recent review,<sup>1</sup> this is the result of a unique combination of properties, which include high melting point, microstructural stability up to temperatures very close to the melting point, excellent chemical stability in oxidizing atmospheres (even in the presence of water vapor). This behavior is associated with an outstanding strength retention at high temperature and creep resistance due to the large area fraction of clean and strong interfaces without glassy phases. While the ambient temperature strength of  $\text{Al}_2\text{O}_3\text{-Y}_3\text{Al}_5\text{O}_{12}$  (YAG) and  $\text{Al}_2\text{O}_3\text{-Er}_3\text{Al}_5\text{O}_{12}$  (EAG) bulk eutectics processed by the Bridgman method

were below 0.5 GPa due to large domain size generated at low growth rates, large improvements were obtained with other growth techniques. For instance,  $\text{Al}_2\text{O}_3\text{-YAG}$  eutectics solidified at high growth rates (750 mm/h) under the high thermal gradients provided by the laser-heated floating zone method presented an ambient temperature strength of 1.9 GPa owing to the fine and homogeneous microstructure formed by an interpenetrating network of submicron domains of both phases.<sup>4</sup> Further reductions in the domain size were obtained by adding a third phase ( $\text{ZrO}_2$ ) to the eutectic mixture, leading to  $\text{Al}_2\text{O}_3\text{-YAG-yttria-stabilized ZrO}_2$  (YSZ) ternary eutectics. They presented higher strength than the binary counterparts grown at the same rate because of their smaller domain size. Finally, nanofibrillar  $\text{Al}_2\text{O}_3\text{-YAG-YSZ}$  ternary eutectics with a bending strength of 4.6 GPa were recently grown at 1200 mm/h, in an inert atmosphere. The microstructure was formed by bundles of single-crystal c-oriented  $\text{Al}_2\text{O}_3$  and  $\text{Y}_3\text{Al}_5\text{O}_{12}$  whiskers of  $\sim 100\text{nm}$  in width with smaller YSZ whiskers between them.

The results summarized above show that large improvements in the strength of DSEO can be achieved by the appropriate changes in the microstructure. Nevertheless, the Achilles heel of DSEO for structural applications is their low toughness, which makes them prone to catastrophic failure. In addition, their strength is very sensitive to the nucleation of defects (for instance, by localized coarsening of the microstructure at high temperature as a result of the reaction with Si-containing species in the environment). The fracture toughness of  $\text{Al}_2\text{O}_3$ -YAG at ambient temperature is  $\ll 2 \text{ MPa}\sqrt{\text{m}}$  and independent of the domain size and orientation (perpendicular or parallel to the growth direction).<sup>11</sup> Slightly higher values, in the range  $4\text{--}5 \text{ MPa}\sqrt{\text{m}}$ , were reported in  $\text{Al}_2\text{O}_3$ -YSZ and  $\text{Al}_2\text{O}_3$ -YAG-YSZ DSEO, and were attributed to the toughening effect of the thermal residual stresses. Only ternary eutectics with a nanofibrillar microstructure have presented a significant increase in toughness perpendicularly to the growth axis.<sup>9</sup> In addition, experimental data on the elevated temperature fracture toughness are only available for  $\text{Al}_2\text{O}_3$ -YAG; such information is critical in materials intended for structural applications at high temperature.

The lack of data on the high temperature toughness of DSEO is mainly due the dimensions of the samples processed by directional solidification. Standard specimens for fracture tests can be machined from samples grown by the Bridgman method but not from rods or plates obtained using other direct solidification techniques, in which the thermal stresses induced by the large longitudinal thermal gradients limit the sample thickness to a few millimetres.<sup>1</sup> Ambient temperature toughness can be estimated from these specimens from the length of the cracks emanating from Vickers indentations, but this technique cannot be extended to elevated temperature. In this paper, a new experimental method to measure the toughness at high temperature in thin rods is presented and applied to  $\text{Al}_2\text{O}_3$ -YAG and  $\text{Al}_2\text{O}_3$ -YAG-YSZ from 300 to 1900 K. The results of the fracture toughness and strength as a function of temperature are discussed in the light of the deformation and failure micromechanisms in the binary and ternary eutectic systems.

## 2. Materials and experimental techniques

$\text{Al}_2\text{O}_3$ -YAG and  $\text{Al}_2\text{O}_3$ -YAG-YSZ DSEO were prepared from commercial powders of  $\text{Y}_2\text{O}_3$  (Aldrich, 99%),  $\text{Al}_2\text{O}_3$  (Aldrich, 99.99%) and 8% yttria-stabilized zirconia (Tosoh Corporation) in the binary (81.5 mol%  $\text{Al}_2\text{O}_3$ , 18.5 mol%  $\text{Y}_2\text{O}_3$ ) and ternary (65 mol%  $\text{Al}_2\text{O}_3$ , 19 mol%  $\text{ZrO}_2$ , 16 mol%  $\text{Y}_2\text{O}_3$ ) eutectic compositions. The powder mixture was milled using a vibratory mill (model MM20000, Restch, Haan, Germany) and fired in air at 1000 °C for 1 h. Precursor rods were prepared by isostatically pressing the powder mixture for 2 min at 200 MPa followed by sintering in a furnace at 1500 °C for 12 h.

Eutectic rods were obtained by directional solidification using the laser-heated floating zone method with a  $\text{CO}_2$  laser. The rods were grown with the molten zone travelling upwards at 350 mm/h (binary) or 300 mm/h (ternary) and without rotation of the crystal and precursor. Each material was grown in two different atmospheres, air (ambient pressure) and nitrogen

(slight overpressure of 0.15–0.25 bar). The final rod diameter was around 1.4–1.6 mm. More details on the growth procedure can be found in the referenced work.

The strength of the rods in the longitudinal direction was measured from 300 to 1900 K by flexure tests carried out in an alumina three-point bend testing fixture of 8.5 mm loading span. The specimen and the loading fixture were placed in a furnace and loaded through two alumina rods connected to the actuator and load cell, respectively, of a servo-mechanical testing machine (model 4505, Instron Ltd., High Wycombe, UK). The specimen was held at the test temperature for 30 min before testing. The tests were performed in air under stroke control at a cross-head speed of 50  $\mu\text{m}/\text{min}$ . The flexure strength was computed from the maximum load in the test according to the Strength of Materials theory for an elastic beam of circular section.

Clearly, no standard fracture specimen can be manufactured from ceramic rods of 1.5 mm in diameter and it was necessary to develop a novel strategy. The basic idea was to carry out three-point bend tests, which can be easily carried out at high temperature, on notched rods (Fig. 1a). The eutectic rods were slightly flattened by polishing with abrasive paper (Fig. 1b) and very sharp notch was made in the rods by means of a fs-pulsed laser. The combination of very short pulses ( $<1 \text{ ps}$ ) and high density of energy per unit area triggers strong non-linear processes within a very localized region on the surface of the materials that culminates in the removal of a thin layer

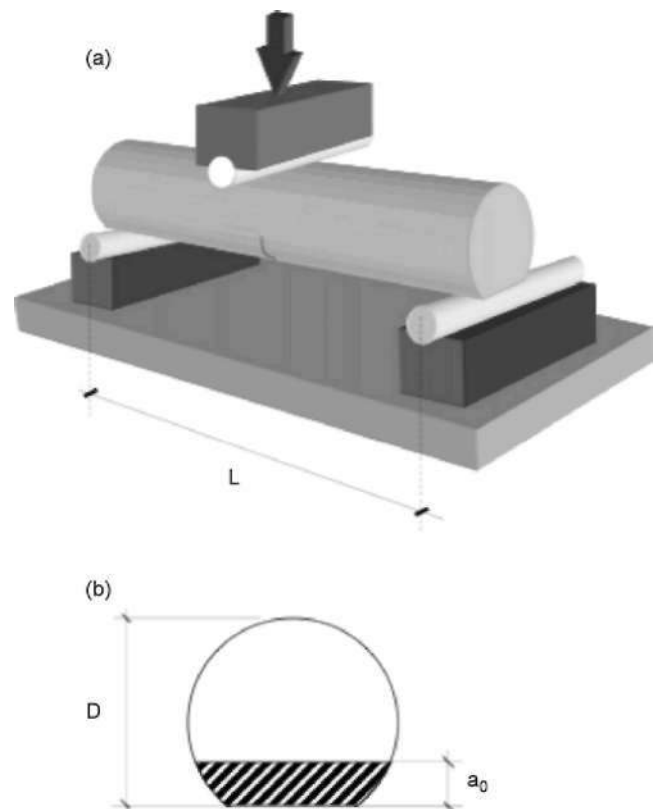


Fig. 1. Schematic of the experimental set-up to carry fracture tests at high temperature on thin rods, (a) Three-point bend fixture and (b) cross-section of the notched rod.

with no time to allow thermal transfer of the absorbed energy to the bulk. This gives rise to spectacular precision and quality of the ablated microstructures without mechanical or thermal damage (Fig. 2). The precise laser processing conditions to make sharp notches in ceramics were previously established for alumina. The stress intensity factor for beam subjected to bending with the section depicted in Fig. 1b was computed from the maximum load in the fracture test and the beam dimensions from the expression provided by Baratta for bending of circular beams with a straight crack. The influence of the flat zone in the circular section was analyzed by Cho who concluded that it was negligible in the case of bending when the initial crack size verified the condition  $ao/D < 0.2$ .

Longitudinal and transversal sections were cut from the rods using a diamond saw, and initially polished using diamond of 30 ( $\mu\text{m}$  grain size as abrasive, and afterwards with a diamond slurry (up to 1 ( $\mu\text{m}$ ). The polished surfaces were coated with a thin layer of Au and the microstructure as well as the fracture surfaces were observed in a scanning electron microscope (Model 6300, Jeol, Tokyo, Japan) equipped with energy-dispersive X-ray microanalysis. Secondary and back-scattered electron detectors were used to ascertain the particular characteristics of the microstructure and the associated fracture micromechanisms (Fig. 2).

### 3. Results and discussion

#### 3.1. Microstructure

The microstructure of the  $\text{Al}_2\text{O}_3$ -YAG DSEO grown in nitrogen in the longitudinal and transversal sections is shown in Fig. 3a and b, respectively. As reported in previous research, the binary eutectic was formed by a three-dimensional interpenetrating network of  $\text{Al}_2\text{O}_3$  (45%) and YAG (55%) domains. The average interlamellar spacing,  $\Lambda$ , (estimated from the transversal back-scattered electron images) was approximately 1.1 ( $\mu\text{m}$ ). The domains were slightly elongated along the growth axis. The microstructure of the ternary DSEO grown in nitrogen is shown in Fig. 4, and presented similar features to the binary counterpart. The material is made of a continuous network of  $\text{Al}_2\text{O}_3$  and YAG domains, which are equiaxed in the transversal section, Fig. 4b, and elongated in the growth direction, Fig. 4a. Smaller YSZ domains, dispersed throughout the microstructure, were nucleated at the boundaries of  $\text{Al}_2\text{O}_3$  and YAG. The average interlamellar spacing,  $\Lambda$ , was 0.7 ( $\mu\text{m}$ ), significantly smaller than that of the  $\text{Al}_2\text{O}_3$ -YAG DSEO, although the growth rates for both materials were very close. This refinement of the domain size due to the presence of the YSZ phase in the eutectic microstructure is well established in the literature. There were no noticeable differences in the microstructure between the materials grown in air and in nitrogen.

#### 3.2. Flexure strength

The average flexure strength of each material, together with the corresponding standard error in the measurements, is plotted in Fig. 5 as a function of the temperature. A minimum of three

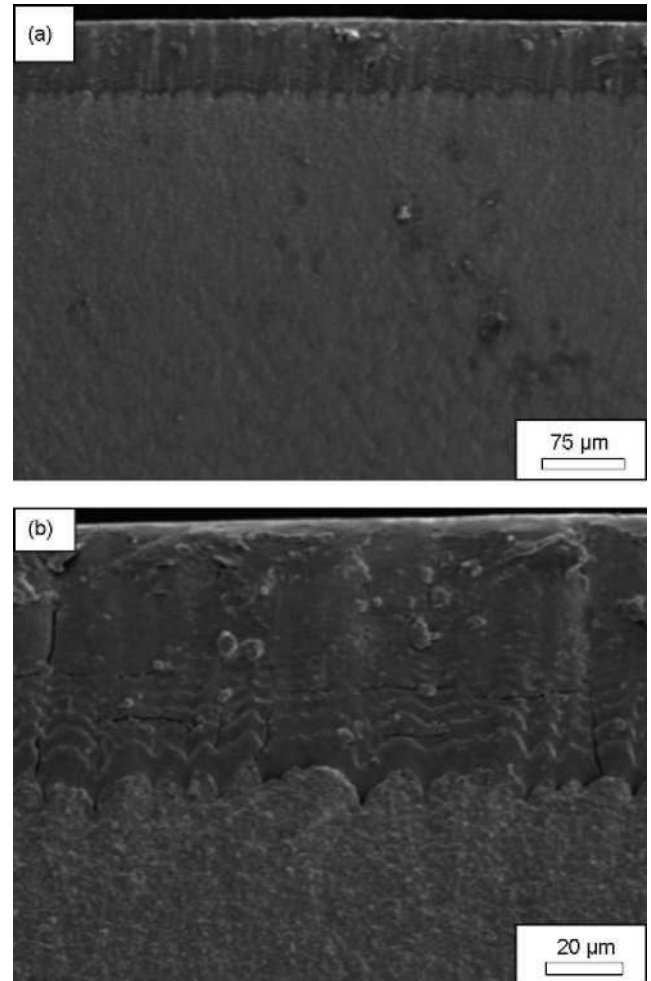


Fig. 2. Fracture surface of a ternary  $\text{Al}_2\text{O}_3$ -YAG-YSZ DSEO tested at 1700 K showing the notch introduced with a fs-pulsed laser and the fracture surface, (a) General view and (b) detail of the notch region.

tests was carried out for each experimental point. These results follow closely the trends established previously in these materials at ambient temperature. The flexure strength is controlled by the critical defect size which depends on the interlamellar spacing in materials with an interpenetrating and homogeneous microstructure. Thus, ternary eutectics present higher ambient temperature strength than the binary counterparts grown at the same rate because of the smaller domain size.

The binary  $\text{Al}_2\text{O}_3$ -YAG DSEO retains most of the ambient temperature strength up to 1900K, very close to the melting point 2099 K. Previous studies in  $\text{Al}_2\text{O}_3$ -YAG DSEO with large interlamellar spacing ( $>20$  ( $\mu\text{m}$ ) have shown that plastic deformation at high temperature and high applied stress is controlled by dislocation motion in YAG phase. This deformation mechanism leads to very high strength retention at high temperature owing to the excellent creep resistance of single-crystal YAG and to the interpenetrating microstructure which imposed similar strain rates in both phases. Parallel studies carried out in binary  $\text{Al}_2\text{O}_3$ -YAG DSEO under creep conditions (applied stresses below 500 MPa and low strain rates) showed that bulk diffusion in YAG becomes the dominant pro-

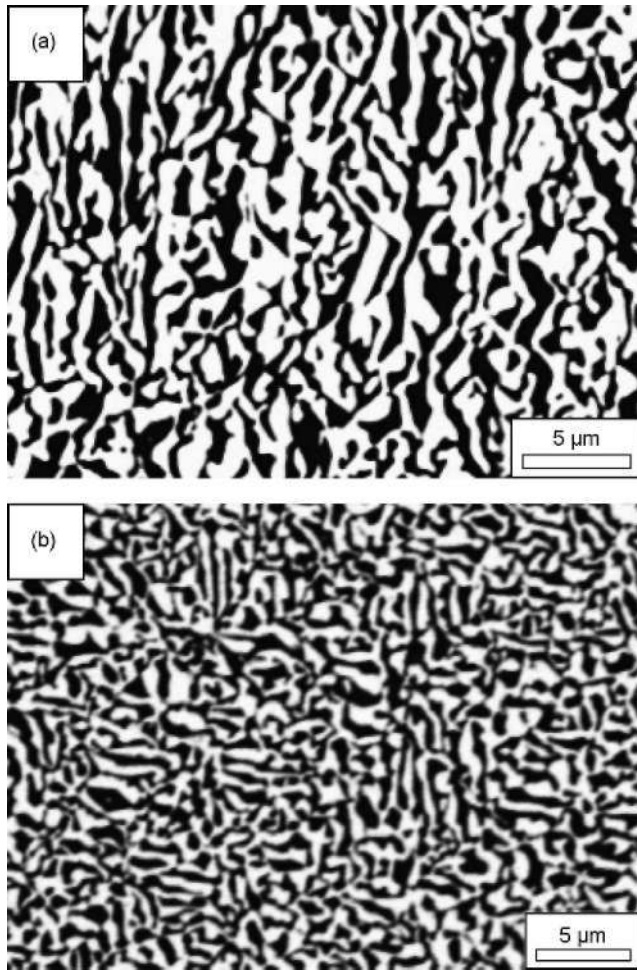


Fig. 3. Back-scattered scanning electron micrographs of the of  $\text{Al}_2\text{O}_3$ -YAG binary eutectic grown in nitrogen at 350 mm/h. (a) Longitudinal section and (b) transversal section. The black phase is alumina, and the white one YAG.

cess of deformation in this situation, and the creep resistance decreases with interlamellar spacing. This effect is, however, very limited in the bending tests carried out in this research which involve high applied stresses and very short time for diffusion, and thus the binary  $\text{Al}_2\text{O}_3$ -YAG DSEO retained the fracture strength at high temperature. In fact, the slight strength reduction at high temperature was attributed to the coarsening of the fine microstructure and the associated growth of the defects rather than to the plastic deformation.<sup>4</sup>

On the contrary, the ternary  $\text{Al}_2\text{O}_3$ -YAG-YSZ DSEO showed a large reduction in strength above 1500K. Several causes have been proposed to explain this behavior,<sup>1</sup> including the smaller domain size and lower eutectic temperature of 1988 K (which enhance diffusion-assisted plastic deformation), the release of thermal residual stresses (which reduce the toughness), and the presence of cubic  $\text{ZrO}_2$  (whose resistance to plastic flow is lower than that of  $\text{Al}_2\text{O}_3$  or YAG). It is very likely that the overall degradation comes about as a result of the contribution of all. For instance, the two latter factors (plastic deformation of YSZ and lower toughness) were responsible for a reduction of 70-80% in strength of  $\text{Al}_2\text{O}_3$ -YSZ DSEO at 1700 K with respect to ambient temperature. This contribution should

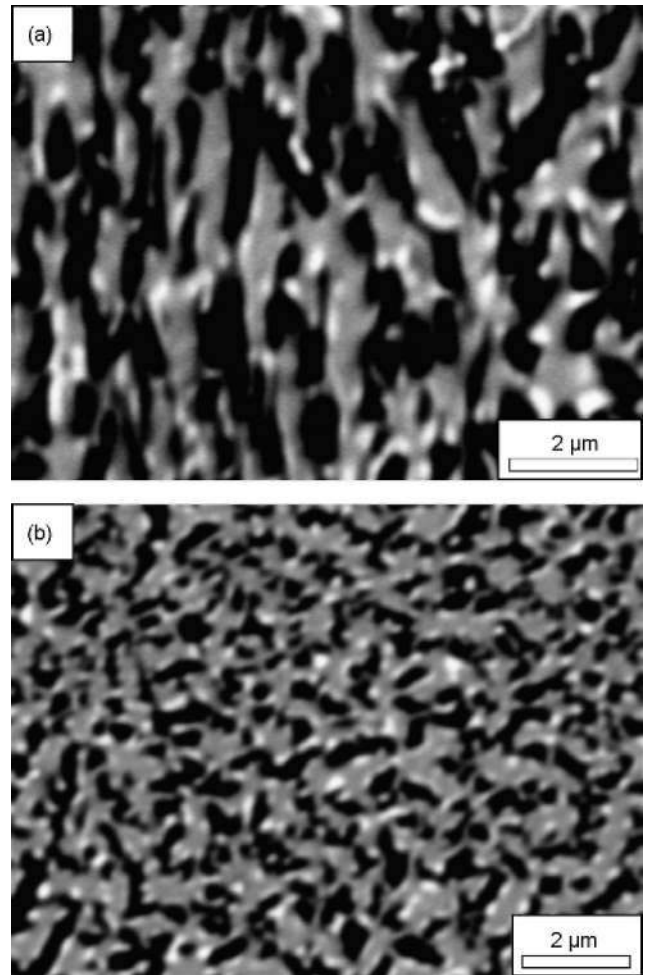


Fig. 4. Back-scattered scanning electron micrographs of the of  $\text{Al}_2\text{O}_3$ -YAG-YSZ ternary eutectic grown in nitrogen at 300 mm/h. (a) Longitudinal section and (b) transversal section. The black phase is alumina, the grey one YAG, and the white one YSZ.

be added to the one provided by the finer microstructure and lower melting temperature in the case of the ternary eutectic.

It should be finally noted that the strength of the DSEO samples grown in nitrogen was consistently higher than that of those grown in air. The influence of the growth rate and atmosphere in the porosity of binary and ternary DSEO manufactured by the laser-heated floating zone method was analyzed by Oliete and Pena.<sup>18</sup> They found that pores develop due to the entrapment of oxygen at the solidification front and, as a result, porosity increases with the growth rate and disappears in samples grown in nitrogen. No pores or bubbles were found in DSEO grown in air at growth rates below 500 mm/h, though the presence of a homogeneous distribution of micropores in the samples grown in air at 300-350 mm/h cannot be ruled out. These pores could act as defects and reduce the strength.

### 3.3. Fracture toughness

The evolution of the fracture toughness with temperature is plotted in Fig. 6a and b for the binary and ternary eutectics.

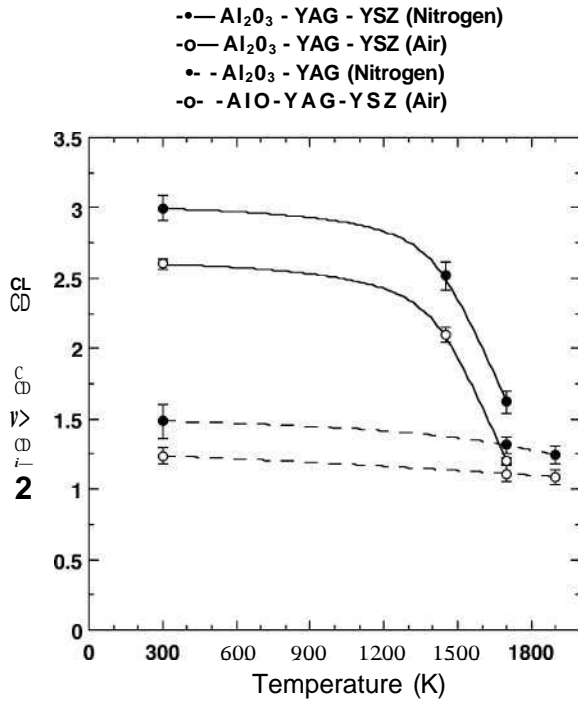


Fig. 5. Flexure strength of the binary ( $\text{Al}_2\text{O}_3$ -YAG) and ternary ( $\text{Al}_2\text{O}_3$ -YAG-YSZ) DSEO grown in air and nitrogen as a function of temperature. The average values and standard errors correspond to a minimum of three tests for each material and temperature.

The average values and standard errors in Fig. 6 correspond to a minimum of three tests for each experimental point. It should be noted that the ambient temperature fracture toughness determined with the technique described in Section 2 is equal to the one obtained with Vickers indentations in binary  $\text{Al}_2\text{O}_3$ /YAG DSEO with the same microstructure and domain size. The fracture toughness of this material was insensitive to the temperature up to  $\sim 1500$  K and increased slightly beyond this point up to  $\sim 4 \text{ MPa}\sqrt{\text{m}}$  at  $1900$  K. Such behavior is corresponds with the results reported by Ochiai and Poza in  $\text{Al}_2\text{O}_3$ /YAG DSEO grown by the Bridgman method with an interlamellar spacing above  $20 \mu\text{m}$ , indicating that the fracture toughness of this material is very insensitive to the microstructure. In addition, samples grown in air or nitrogen presented the same behavior.

Regardless of the temperature, the fracture surfaces were macroscopically smooth and the extremely brittle nature of this material is clearly seen in the straight propagation of the crack through the eutectic domains (Fig. 7). At the microscopic level, the specimens tested at high temperature showed a homogeneous coarsening of the microstructure: the faceted interfaces between  $\text{Al}_2\text{O}_3$  and YAG became rounded and the average interlamellar spacing increased (Fig. 8). In addition, micron-sized pores were nucleated from  $\text{Al}_2\text{O}_3$ /YAG interfaces and were attributed to the stress concentrations generated by the incompatibilities in the plastic deformation of the  $\text{Al}_2\text{O}_3$  and YAG single crystalline domains. Obviously, the energy dissipated by plastic deformation was responsible for the increment in toughness at high temperature.

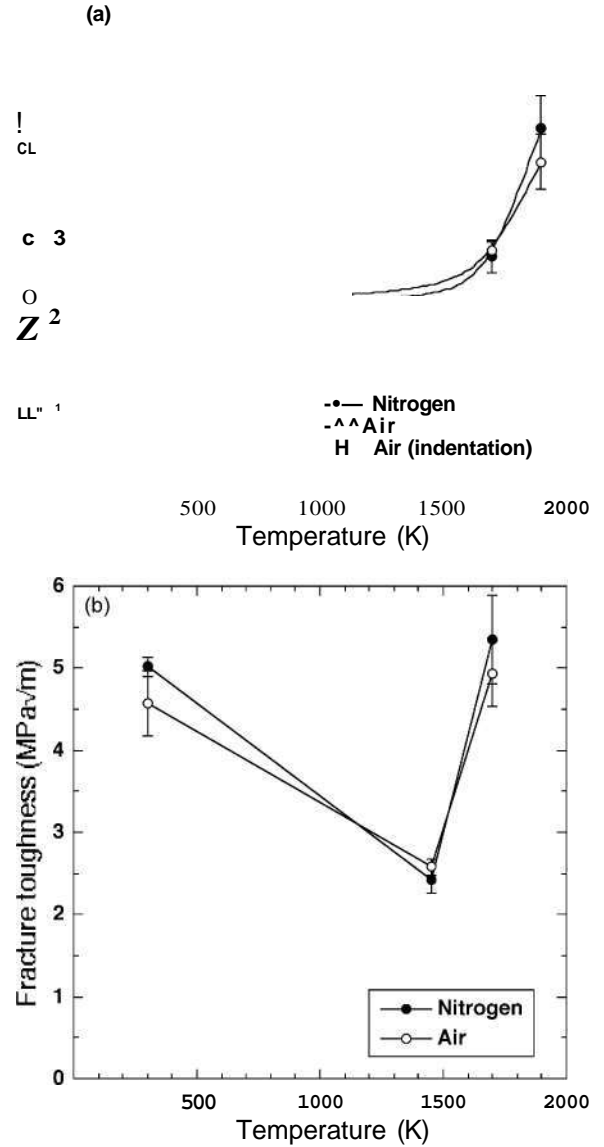


Fig. 6. Fracture toughness of the DSEO grown in air and nitrogen as a function of the temperature, (a) Binary  $\text{Al}_2\text{O}_3$ -YAG and (b) ternary  $\text{Al}_2\text{O}_3$ -YAG-YSZ. The average values and standard errors correspond to a minimum of three tests for each material and temperature. The ambient temperature toughness obtained from Vickers indentations in the  $\text{Al}_2\text{O}_3$ -YAG binary system is also plotted in (a).

The evolution of the fracture toughness of the ternary  $\text{Al}_2\text{O}_3$ -YAG-YSZ DSEO with temperature is plotted in Fig. 6b, and shows significant differences with the binary counterpart. The ambient temperature toughness measured with the notches machined with fs-pulsed laser was similar to those obtained from Vickers indentations in other investigations, and more than twice the values measured in the  $\text{Al}_2\text{O}_3$ -YAG DSEO. These differences were attributed to the thermal residual stresses, which develop upon cooling in the ternary eutectic as a result of the differences in the thermal expansion coefficient of YSZ on the one hand and  $\text{Al}_2\text{O}_3$  and YAG on the other. Residual stresses in the alumina phase of  $\text{Al}_2\text{O}_3$ -YSZ and  $\text{Al}_2\text{O}_3$ -YAG-YSZ DSEO have been measured in previous investigations and the

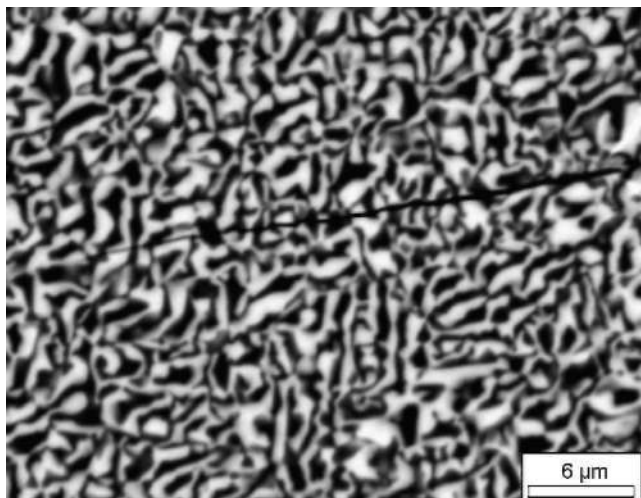


Fig. 7. Crack propagation at ambient temperature in the binary  $\text{Al}_2\text{O}_3$ -YAG DSEO grown in air.

residual stresses in each phase were computed through the self-consistent model. They have shown that the  $\text{Al}_2\text{O}_3$  and YAG domains in the ternary eutectic are subjected to compressive stresses of approximately 200 and 300 MPa, respectively, while

YSZ is under tension ( $>1$  GPa). During crack propagation, the crack front will prefer to rest in regions of compressive stress and in order to continue the crack propagation, the applied stress intensity factor will require increase by an amount equal to the shielding effect induced by the compressive residual stresses at the crack tip.

This hypothesis for the higher toughness of the ternary eutectic at ambient temperature is supported by the results in Fig. 6b at 1500K. The thermal residual stresses are released and fracture toughness drops to the values measured in the binary, residual stress free, DSEO. Ternary eutectics tested at 1700 K showed a sharp increase in toughness which could be attributed to plastic deformation around the crack tip, as in the binary material tested at the same temperature. The fracture surfaces were macroscopically smooth in the ternary eutectic tested at high temperature (Fig. 2) and evidence of plastic deformation at the microscopic level could not be obtained because of the extremely fine size of the domains. Nevertheless, the significant reduction in bending strength and the sharp increase in toughness above 1500K seem to be a result of the development of diffusion-assisted plastic flow. It should be finally noted that samples grown in air or nitrogen presented the same behavior.

#### 4. Conclusions

The flexure strength and the fracture toughness of binary ( $\text{Al}_2\text{O}_3$ -YAG) and ternary ( $\text{Al}_2\text{O}_3$ -YAG-YSZ) DSEO grown by the laser-heated floating zone method were measured from ambient temperature up to 1900K. The ambient temperature strength was primarily a function of the interlamellar spacing, which controlled the critical defect size, and the ternary eutectics were stronger than the binary. The fracture behavior at ambient temperature was very brittle, and the cracks propagated in straight line through the domains in the  $\text{Al}_2\text{O}_3$ -YAG eutectic. The compressive thermal residual stresses in the  $\text{Al}_2\text{O}_3$  and YAG domains of ternary eutectic improved slightly the ambient temperature toughness.

The mechanical properties of the  $\text{Al}_2\text{O}_3$ -YAG binary eutectic did not change with temperature up to 1500-1600 K. The activation of plastic deformation mechanisms above this temperature led to a slight reduction in the strength and an increase in toughness. In the case of the ternary eutectic, the toughening effect of the thermal residual stresses disappeared at high temperature: the fracture toughness at 1473 K was reduced by a factor of two, and it was equivalent to that of  $\text{Al}_2\text{O}_3$ -YAG. The behavior of the ternary eutectic above this temperature followed the trends of the binary one: increase in toughness and reduction in strength. The changes were, however, much more significant because the smaller domain size and the lower eutectic temperature of the ternary eutectic promoted the activation of diffusion-assisted plastic deformation.

#### Acknowledgements

The authors gratefully acknowledge the financial support from the Ministerio de Education y Ciencia de Espana under

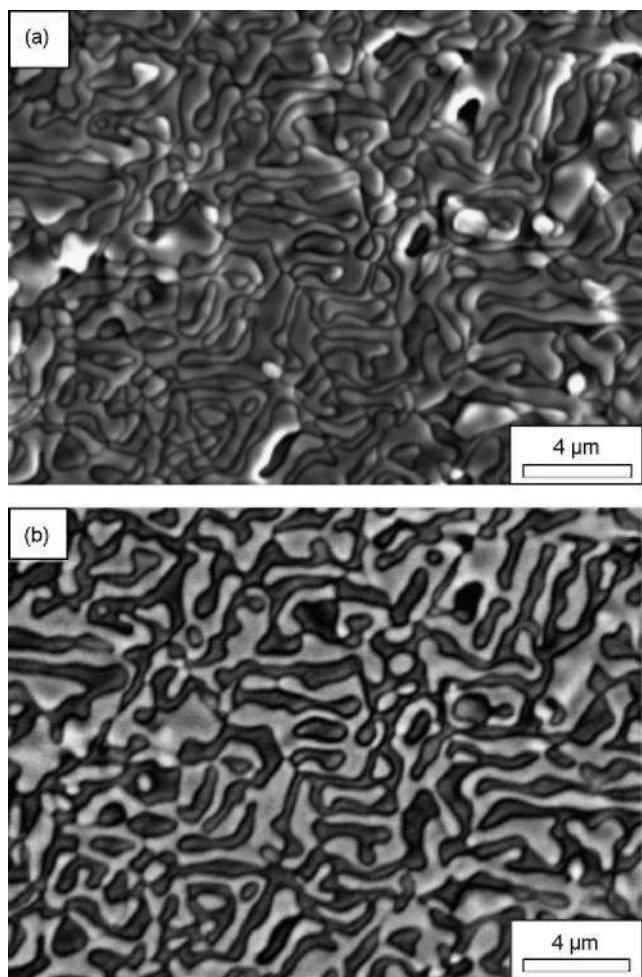


Fig. 8. Fracture surface of the  $\text{Al}_2\text{O}_3$ -YAG DSEO tested at 1900 K. (a) Secondary electron image and (b) back-scattered electron image.

project MAT2006-13005 and from the Comunidad de Madrid through the program ESTRUMAT-CM.

## References

- Llorca, J. and Orera, V. M., Directionally solidified eutectic oxide ceramics. *Prog. Mater. Sci.*, 2006, **51**, 711-809.
- Waku, Y., Ohtsubo, H., Nakagawa, N. and Kohtoku, Y., Sapphire matrix composites reinforced with single crystal YAG phases. *J. Mater. Sci.*, 1996, **31**, 4663-4670.
- Waku, Y., Nakagawa, N., Ohtsubo, H., Mitani, A. and Shimizu, K., Fracture and deformation behaviour of melt growth composites at very high temperatures. *J. Mater. Sci.*, 2001, **36**, 1585-1594.
- Pastor, J. Y., Llorca, J., Salazar, A., Oliete, P. B., de Francisco, I. and Peiia, J. I., Mechanical properties of melt-grown alumina-YAG eutectics up to 1900 K. *J. Am. Ceram. Soc.*, 2005, **88**, 1488-1495.
- Matson, L. E. and Hecht, N., Microstructural stability and mechanical properties of directionally solidified alumina/YAG eutectic monofilaments. *J. Eur. Ceram. Soc.*, 1999, **19**, 2487-2501.
- Waku, Y., Sakata, S., Mitani, A., Shimizu, K. and Hasebe, M., Temperature dependence of flexural strength and microstructure of Al<sub>2</sub>O<sub>3</sub>-Y<sub>3</sub>Al<sub>5</sub>O<sub>12</sub>-ZrO<sub>2</sub> ternary melt growth composites. *J. Mater. Sci.*, 2002, **37**, 2975-2982.
- Pena, J. I., Larsson, M., Merino, R. I., de Francisco, I., Orera, V. M., Llorca, J., Pastor, J. Y., Martin, A. and Segurado, J., Processing, microstructure and mechanical properties of directionally-solidified Al<sub>2</sub>O<sub>3</sub>-Y<sub>3</sub>Al<sub>5</sub>O<sub>12</sub>-ZrO<sub>2</sub> ternary eutectics. *J. Eur. Ceram. Soc.*, 2006, **26**, 3113-3121.
- Lee, J. H., Yoshikawa, A., Fukuda, T. and Waku, Y., Growth and characterization of Al<sub>2</sub>O<sub>3</sub>/Y<sub>3</sub>Al<sub>5</sub>O<sub>12</sub>/ZrO<sub>2</sub> ternary eutectic fibers. *J. Cryst. Growth*, 2001, **231**, 115-120.
- Oliete, P. B., Pena, J. I., Larrea, A., Orera, V. M., Llorca, J., Pastor, J. Y., Martin, A. and Segurado, J., Ultra-high strength nanofibrillar Al<sub>2</sub>O<sub>3</sub>-YAG-YSZ eutectics. *Adv. Mater.*, 2007, **19**, 2313-2318.
- Yang, J.-M., Yeng, S. M. and Chang, S., Fracture behavior of directionally solidified Y<sub>3</sub>Al<sub>5</sub>O<sub>12</sub>/Al<sub>2</sub>O<sub>3</sub> eutectic fiber. *J. Am. Ceram. Soc.*, 1996, **79**, 1218-1222.
- Ochiai, S., Ueda, T., Sato, K., Hojo, M., Waku, Y., Nakagawa, N., Sakata, S., Mitani, A. and Takahashi, T., Deformation and fracture behavior of an Al<sub>2</sub>O<sub>3</sub>/YAG composite from room temperature to 2023 K. *Compos. Sci. Technol.*, 2001, **61**, 2117-2128.
- Pastor, J. Y., Poza, P., Llorca, J., Peiia, J. I., Merino, R. I. and Orera, V. M., Mechanical properties of directionally solidified Al<sub>2</sub>O<sub>3</sub>-ZrO<sub>2</sub>(Y<sub>2</sub>O<sub>3</sub>) eutectics. *Mat. Sci. Eng. A*, 2001, **308**, 241-249.
- Echigoya, J., Takabayashi, Y. and Suto, H., Hardness and fracture toughness of directionally solidified Al<sub>2</sub>O<sub>3</sub>-ZrO<sub>2</sub>(Y<sub>2</sub>O<sub>3</sub>) eutectics. *J. Mater. Sci.*, 1986, **5**, 153-154.
- Larrea, A., de laFuente, G. F., Merino, R. I. and Orera, V. M., ZrO<sub>2</sub>-Al<sub>2</sub>O<sub>3</sub> eutectic plates produced by laser zone melting. *J. Eur. Ceram. Soc.*, 2002, **22**, 191-198.
- Hirano, K., Application of eutectic composites to gas turbine system and fundamental fracture properties up to 1700°C. *J. Eur. Ceram. Soc.*, 2005, **25**, 1191-1199.
- Calderon-Moreno, J. M. and Yoshimura, M., Microstructure and mechanical properties of quasi-eutectic Al<sub>2</sub>O<sub>3</sub>-Y<sub>3</sub>Al<sub>5</sub>O<sub>12</sub>-ZrO<sub>2</sub> ternary composites rapidly solidified from the melt. *Mat. Sci. Eng. A*, 2004, **375-377**, 1250-1254.
- LLorca, J., Pastor, J. Y., Poza, P., Peiia, J. I., de Francisco, I., Larrea, A. and Orera, V. M., Influence of the Y<sub>2</sub>O<sub>3</sub> content and temperature on the mechanical properties of melt-grown Al<sub>2</sub>O<sub>3</sub>-ZrO<sub>2</sub> eutectics. *J. Am. Ceram. Soc.*, 2004, **87**, 633-639.
- Oliete, P. B. and Peiia, J. I., Study of the gas inclusions in Al<sub>2</sub>O<sub>3</sub>/Y<sub>3</sub>Al<sub>5</sub>O<sub>12</sub> and Al<sub>2</sub>O<sub>3</sub>/Y<sub>3</sub>Al<sub>5</sub>O<sub>12</sub>/ZrO<sub>2</sub> fibers grown by laser floating zone method. *J. Cryst. Growth*, 2007, 514-519.
- Pastor, J. Y., Martin, A., Llorca, J., Moreno, P., Mendez, C., Campos, J. L., Garcia, A. and Arias, I. *J. Am. Ceram. Soc.*, in preparation.
- Stuart, B. C., Feit, M. D., Herman, S., Rubenchik, A. M., Shore, B. W. and Perry, M. D., Optical ablation by high-power short-pulse lasers. *J. Opt. Soc. Am. B*, 1996, **13**, 459-472.
- Gamaly, E. G., Rode, A. V., Luther-Davies, B. and Tikhonchuk, V. T., Optical ablation by high-power short-pulse lasers. *Phys. Plasmas*, 2002, **9**, 949-957.
- Baratta, F. I., Wide range stress intensity factors for straight-fronted edge crack in a three-point bend, round bar specimen. *Int. J. Fract.*, 1993, **60**, R59-R63.
- Cho, K., Hantzand, B. F. and Bar-on, I., Stress intensity factor calculation for modified round bend bar by 3-D finite element analysis. *Int. J. Fract.*, 1993, **62**, 163-170.
- Harada, Y., Suzuki, T., Hirano, K. and Waku, Y., Ultra-high temperature compressive creep behavior of an in-situ Al<sub>2</sub>O<sub>3</sub> single crystal/YAG eutectic composite. *J. Eur. Ceram. Soc.*, 2004, **24**, 2215-2222.
- Matson, L. E. and Hecht, N., Creep of directionally solidified alumina/YAG eutectic monofilaments. *J. Eur. Ceram. Soc.*, 2005, **25**, 1225-1239.
- Ramirez-Rico, J., Pinto-Gomez, A. R., Martinez-Fernandez, J., de Arellano-Lopez, A., Oliete, P. B., Peiia, J. I. and Orera, V. M., High-temperature plastic behaviour of Al<sub>2</sub>O<sub>3</sub>/Y<sub>3</sub>Al<sub>5</sub>O<sub>12</sub> directionally solidified eutectics. *Acta Mater.*, 2006, **54**, 3107-3116.
- Poza, P., Pastor, J. Y., Llorca, J. and Waku, Y., Comportamiento en fractura de un eutectico Al<sub>2</sub>O<sub>3</sub>-YAG crecido por solidificacion direccional. *Bol. Soc. Esp. Ceram. V*, 2006, **45**, 401-407.
- Pardo, J. A., Merino, R. I., Orera, V. M., Peiia, J. I., Gonzalez, C., Pastor, J. Y. and Llorca, J., Piezospectroscopic study of residual stresses in Al<sub>2</sub>O<sub>3</sub>-ZrO<sub>2</sub>(Y<sub>2</sub>O<sub>3</sub>) directionally solidified eutectics. *J. Am. Ceram. Soc.*, 2000, **83**, 2745-2752.
- Orera, V. M., Merino, R. I., Pardo, J. A., Larrea, A., Peiia, J. I., Gonzalez, C., Poza, P., Pastor, J. Y. and Llorca, J., Microstructure and physical properties of some eutectic composites processed by directional solidification. *Acta Mater.*, 2000, **48**, 4683-4689.
- Harlan, N. R., Merino, R. I., Peiia, J. I., Larrea, A., Orera, V. M., Gonzalez, C., Poza, P. and Llorca, J., Phase distribution and residual stresses in melt-grown Al<sub>2</sub>O<sub>3</sub>-ZrO<sub>2</sub>(Y<sub>2</sub>O<sub>3</sub>) eutectics. *J. Am. Ceram. Soc.*, 2002, **85**, 2025-2032.